Journal of Radiation and Nuclear Applications
An International Journal

http://dx.doi.org/10.18576/jrna/090307

Investigation of Neutron Attenuation Capability of Different Clay Materials

Samy.A.Dwidar[1*], *Rowayda. Fayez*[1] *and Mohamed. Elsafi*[2]

[1]Egyptian Atomic Energy Authority.
[2]physics Department , Faculty of Science, Alexandria University.

Received: 2 Jun. 2024, Revised: 22 Jul. 2024, Accepted: 1 Aug. 2024.

Published online: 1 Sep 2024

Abstract: This research intends to develop various shielding materials to shield employees and general public from the effects of neutron radiation. The Monte Carlo N-Particle (MCNP) transport algorithm is used to predict the neutron macroscopic cross section (or neutron attenuation) for three samples of distinct clays (ball clay, kaolin, and betonies). Simultaneously an experimental work with the aide of the neutron source Plutonium-Alpha-Beryllium (Pu-α-Be) is done to measure the neutron flux and the neutron macroscopic cross section in order to verify the theoretical results. In the current study, a number of kinds of Egyptian clays are regarded as a natural construction materials have been examined as radiation shielding materials. The microstructure of these samples was examined using scanning electron microscopy. These sorts of construction materials have excellent chemical durability, In addition to being naturally available; they also have a low hydraulic conductivity and a reasonably high hardness. Compared to other shielding materials, the clays are good resistant to chemicals and environment factors and are more readily available in Egypt.

Keywords: Neutron attenuation, Clay, Neutron cross sections, and MCNP.

1 Introduction

Neutrons and other forms of ionizing radiation are extremely harmful to human health, thus it is important to evaluate the hazards, evaluate the exposure threshold, and create protective technology. [1]. Because neutrons only interact with matter through nuclei, it is difficult to stop passing through most materials and they can travel great distances through them without scattering or absorbing, which makes neutron shielding a complex process. This indicates that the neutrons are harmful in terms of material and radiation because of their great penetrability ability.

[2], the main parameters characterize the way neutrons interact with matter are as removal cross-section(Σ_R),mean free path, and half thickness [3]. The shielding system's goals are to reduce radiation exposure and attenuate neutron particles. [4]. the way that neutrons interact with materials is different from that of photons because being neutral, they do not carry a charge therefor can enter nuclei [5].

The kinetic energy of the neutrons is primarily responsible for how neutron radiation interacts with materials through atoms' nuclei. Neutrons categorized by energy are three types in general. Thermal neutrons (less than 1 eV), Epithermal neutrons (between 1 eV and 0.1 MeV), and Fast neutrons (over 0.1 MeV), the flounce is used to express the amount of neutron radiation absorbed in materials. The neutron flounce is defined as the number of neutrons (n) per unit area, as (n/cm2). when measure the neutron radiation rate it is expressed in terms of flux, or (n/cm2/s).

It is necessary to slow down fast and intermediate neutrons and then absorb thermal neutrons when designing the neutron shields. Thus, For shielding purpose the overall composition of a material containing atoms that can thermalize and absorb neutrons is essential.[6].

The mechanism of reaction between neutrons and nuclei involves. (Elastic and inelastic) scattering and absorption. In elastic scattering interactions, the nucleus tends to be stable and subject to the loss of momentum and energy maintenance. Whereas the inelastic scattering interactions leave the nucleus in an excited state following the reaction, and they are followed with the return of the exciting

*Corresponding author e-mail: samydwidar@yahoo.com

nucleus into the ground stable through the emission of gamma rays. [7]. regarding reactions of absorption, the nucleus absorbs and captures the neutron, which causes the nucleus to transform into an unstable radioactive nucleus. The nucleus then releases excess energy in the form of gamma rays in order to stabilize. [8],

In the present study, certain Egyptian clay varieties that are employed as natural building materials have been examined for their potential as neutron shielding materials. The current clays are clean and sustainable building materials that may be added to concrete mixtures in precise ratios to raise their density and improve neutron attenuation. They can also be utilized as a neutron shield in radiation protection applications.

1.1 Computational methods

The Monte Carlo algorithm is one of the recent computer techniques that have become essential for producing radiation-shielding composites for nuclear uses. With these methods, radiation calculations in complicated three-dimensional geometries may be completed quickly and precisely. In addition to determine the best materials' chemical composition for maximum attenuation, Mechanical and physicochemical characteristics are determined for a particular application. Some of the advantages of using computational techniques are:

(1) Provides sensitivity analysis and optimization for real systems without the need to operate those systems in real time.
(2) Simulated experimental conditions are more strictly regulated than what the real system is.

(3) Analyzing the system for a longer or shorter time frame is simple than its actual operation.

The Monte Carlo approach is employed in particle physics. Which simulates how radiation moves through materials? Add to that, the Monte Carlo method gets realistic solutions for the transport equation over 3D complicated geometry because the transport equation cannot be analytically solved for a number of real-world situations. The Monte Carlo method involves using a synthetic random number generator to simulate the histories of a certain number of particles through interactions with matter. [9]. Random numbers are created and utilized to sample the proper probability distributions for each particle history, including those for the particle/photon's starting energy, path of motion, step duration, interacting nucleus, what kind of interaction, subsequent direction, etc. It is possible to determine the expectation or mean value $\bar{x}$ of various quantities, which might include the flux, current, escape probability, or any number of different quantities, through tracking every particle's history. The answer provided by this method, which is primarily based on statistical ideas, is not unique; rather, it is an estimate that should fall within specific intervals of confidence for the "true" answer. As there are more histories, there is less uncertainty about the final result.

Several studies have utilized Monte Carlo simulations to examine the attenuation properties of the concrete. Most of the published research concentrated on looking the gamma ray attenuation coefficients in concretes containing iron and lead [10]. [11]. & additional mineral additives investigated the gamma shielding qualities of concretes with varied hematite percentages using numerical simulations utilizing the Monte Carlo N-Particle code (MCNP). [13]. [14]. Different concrete compositions containing boron and improvement polymers have also been the subject of computational studies of neutron shielding. [15].[16]. Utilizing the FLUKA Monte Carlo simulation system, the neutron attenuation properties are examined for concrete enriched in Ferro boron as well as boron carbide [17]. [18] In addition conduct researches on the significance of cement-based composites' atomic compositions and moisture content in neutron shielding is studied with Monte Carlo simulation using the FLUKA code

Investigation on the concrete's ability to shield hadron-therapy accelerators also has been studied [19]. All these Simulation works are firmed up by experimental evidence showing excellent agreement between the two techniques.

2 Material and methods

2.1 Sample preparation

Three different types of clay, including, ball clay, kaolin, and bentonite, have been obtained from quarries in the Egyptian provinces of Aswan, Abuznima, and Fayoum. They were stoned, reduced to powder, and dried in the sun. After being sieved to a size of 100 m, the materials had been thoroughly mixed with water and dried in the sun after splitting into sections. After that, the samples were baked at a temperature of 500oC. The A, B and C, respectively, are samples of, ball clay, kaolin, and bentonite are shown in Figure (1). The formula used to determine the porosity, P, of the sample, which is referred to as the ratio of the void volume with the total volume is. [20-23].

$$P\ (\%) = \frac{W-D}{V}$$

Where W (g), is the saturated mass of clay sample (the sample immersed in boiling water for 2 h), D (g), is the dried mass of clay sample (the sample dried in the oven at 110 ^{0}C for 48 h) and V (cm3) is the exterior (total) volume of the sample (V = W × S), where S (g), is the suspended weight of sample in water.

Fig. 1: The various clay samples that was prepared.

Figure (2) illustrates the distribution of particles inside each type of clay viewed using a scanning electron microscope (SEM).

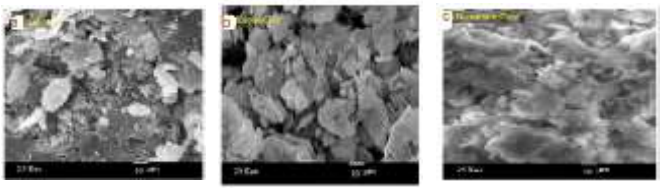

Fig. 2: SEM images for the various clays that are dealt with in this study where (a) ball clay (b) kaolin and (c) Bentonite.

The flowing table illustrates the chemical compositions of clay samples.

Table 1. The chemical compositions of four different clays and their density.

Sample Red Clay	Ball Clay 1.99 g/cm3	Kaolin 1.99 g/cm3	Bentonite 2.1 g/cm3
Na2O	0	0	1.3 ± 0.11
MgO	0	2.99 ± 0.16	1.18 ± 0.21
Al2O	35.08 ±0.21	35.53 ± 0.24	20.35 ± 0.14
SiO2	58.26 ± 0.21	55.26 ± 0.11	49.65 ± 0.22
SO3	0	0	1.96 ± 0.46
K2O	0	0	1.28 ± 0.13
CaO	0	1.24 ± 0.42	10.92 ± 0.25
TiO2	2.5 ± 0.21	2.76 ± 0.25	2.74 ± 0.14
FeO	4.16 ± 0.21	2.22 ± 0.17	10.62 ± 0.19

Figure (3) depicts a schematic of the experimental setup utilised for the neutron propagation measurements as well as its geometrical details. The measurements were performed using the fast neutrons emitted by Pu-α-Be (plutonium –alpha- prelium) source with activity 5 Ci and half-life of 24360 years

. To protect against emanating γ-rays, the fast neutron beam was extracted using a lead shielding directly behind the source. A stilpene-organic scintillator detector was used to count the neutrons over a 30-minute period. As shown in Figure (3), the detector was placed 30 cm apart from the sample for all measurements. The Lambert-Beer equation was used to determine the macroscopic cross section (Σ, $cm-1$) for each sample:

$$\sum(E) = -\frac{1}{x}\ln\left(\frac{I(E)}{I_0(E)}\right) \quad (1)$$

Where x is the sample's thickness, I_o and I, are the incident and transmitted beam intensities respectively. There was no shielding sample present when the incidence intensity was measured (which is called the bare sample).

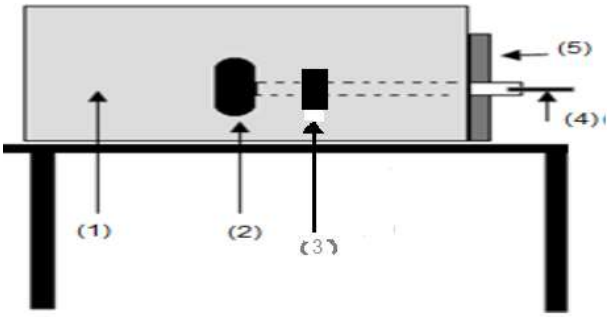

Fig. 3: The set-up schematic diagram used in the current work.

Where,
1-Shield of paraffin
2-Neutron source
3- Sample
4 –Stilpene scintillator detector
5-Arounding detector shield of paraffin

2.2 The macroscopic cross sections of fast neutrons (Σ):

This parameter, denoted by Σ describes the probability of interaction of a neutron with a target material with units of cm^{-1}. Where the fast neutrons can, however, undergo a number of interactions with the nuclei's which are required in shielding study they are known four neutron interaction modes [22].

1- Elastic scattering: Neutrons are slowed down by interacting with atomic nuclei primarily by Moderation according to this equation.
2- The average energy loss

$$= \frac{2EA}{(A+1)}$$

(2)

Where the average energy loss occurs when the incident neutron with kinetic energy E strikes an atomic nucleus with atomic weight A.
2- Inelastic scattering: often occurred by heavy materials to slow down the neutrons through this equation.

$$E' = 6.4\sqrt{\frac{E}{A}} \quad (3)$$

Where E is the energy of the incident neutron, and E' is the energy of a neutron emerging from an inelastic scattering.

3-Transmutation: In this type of reaction the element transforms into another when a neutron is absorbed by a nucleus.

4-Radioactive Capture: This reaction has low absorption cross section with fast neutron where a nucleus absorbs the neutron and enters an excited state. The nucleus releases gamma rays to get back to its stable state. The equation represents this reaction is

$$n + X_p{}^{n+p} \rightarrow X_p{}^{n+p+1} + \gamma \quad (4)$$

2.3 Mathematical Model

The simulations were carried out using version 6 of the Monte Carlo N-Particle Transport Code. (MCNP6) developed at the Los Alamos National Laboratory [12]. The transport code MCNP6 is used to simulate how neutron radiation interacts with matter. The geometrical model utilized in MCNP simulations is depicted in Figure (6).Where Monte Carlo code (MCNP6) was used to model the experiment in order to calculate the attenuation coefficient of neutron radiation or total macroscopic cross section (Σ) for each one of the three different samples (ball clay, kaolin and bentonite) by tally F8. The source used in MCNP6 is general source (SDEF) that is defined with the required energy range, position, and type of particle.

Finally to validate, and check the accuracy of the theoretical results we compare it with the experimental results.

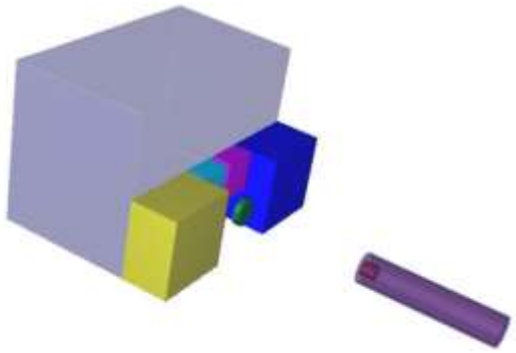

Fig. 6: The simulated experiment by VISED MCNP6.

Figure. (7) Depict the neutron spectrum used in MCNP simulation.

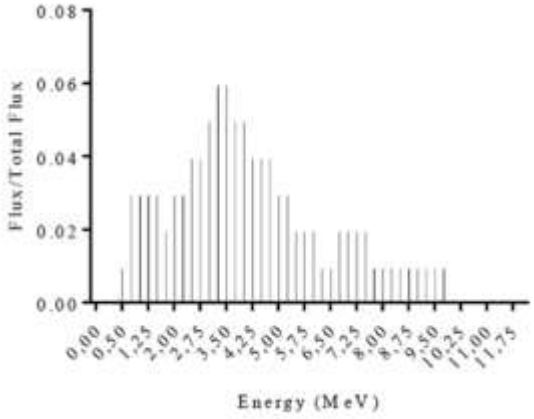

Fig.7: The energy distribuotin of the source.

4 Results and Discussion

Figure. 8 (a, b, c) displays the exponential neutron fluxes of the three samples. The investigated flux of the three samples are plotted with an energy range of (0.8 -7 MeV).

Figure. 8 (a) shows that the neutron flux has been attenuated by the ball clay sample mostly as a result of inelastic scattering by the component elements-with high density- as iron, calcium, silicon, and titanium or by radioactive capture by sodium and aluminum as mentioned by equations (3) , (4)

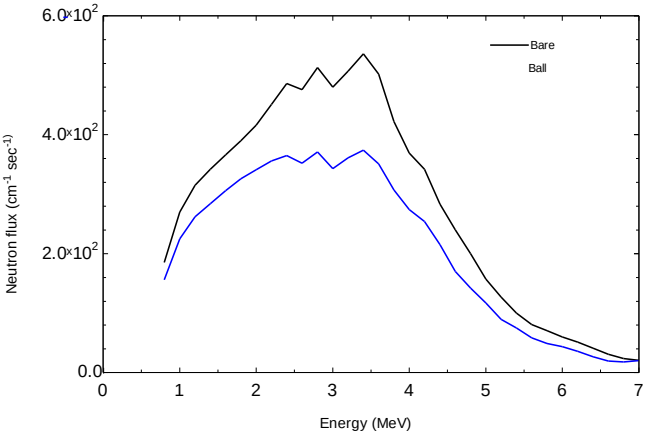

Fig.8-a Fast neutron flux spectra behind ball clay barrier.

Figure. (8-b) demonstrates the neutron flux has been attenuated by the kawlin sample also as a result of inelastic scattering by the component elements-with high density- as iron, calcium, silicon and titanium or by radioactive capture by sodium and aluminum. There is a difference from the ball clay case and this is attributed to the difference of concentrations of elements composite the sample.

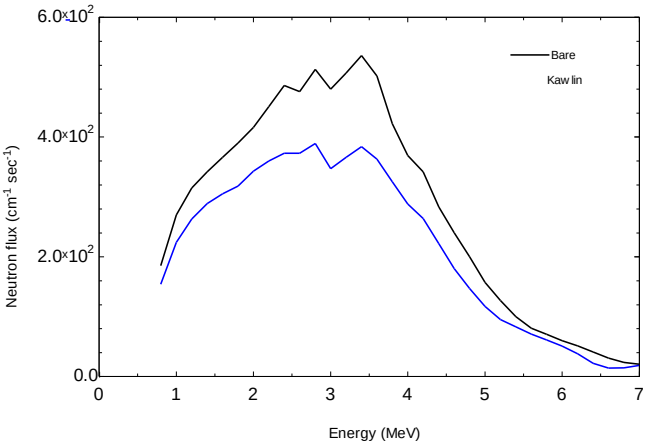

Fig. (8-b) Fast neutron spectra behind kawlin barrier

Figure. (8.c) also illustrates the neutron flux attenuated by the Bentonite sample as a result of inelastic scattering by the component elements-with high density-as iron, calcium, silicon and titanium or by radioactive capture by sodium and aluminum. There is a difference from the above two cases due to the difference of concentrations of the elements of composition of this sample from the above two.

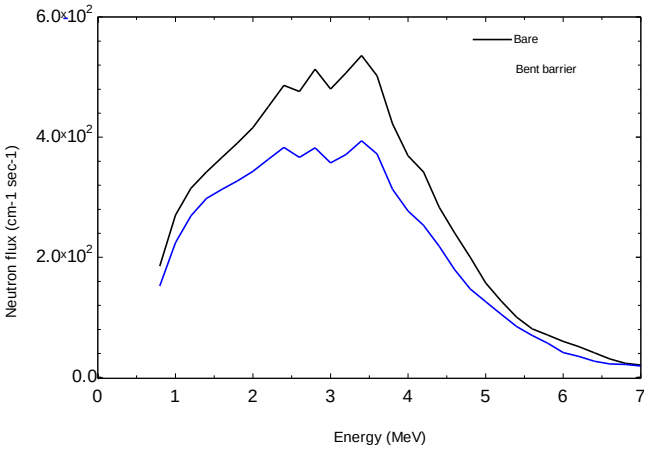

Fig. (8.c): Fast neutron flux spectra behind Bentonite barrier.

4.1 The results of comparison

The total macroscopic cross section of fast neutron (Σ) has been calculated using equation (1) by MCNP simulation for various samples and confirmed with experiment measurements in parallel as follow:

a.sample # 1 (Ball clay) by MCNP simulation

Name	Ball clay
NPS	5E8
Temp.	Room temp
Thickness	2.95cm

(Where NPS is the number of particles-including runs)

Figure. (9.a) demonstrates the total macroscopic cross section of fast neutron (Σ) which have been calculated by MCNP simulations and measured experimentally for ball clay shields. The total cross is mostly due to inelastic scattering by high density element such as iron through equation (3). It is observed that the total cross section mostly depends on the inelastic scattering type of the elements composing shields.

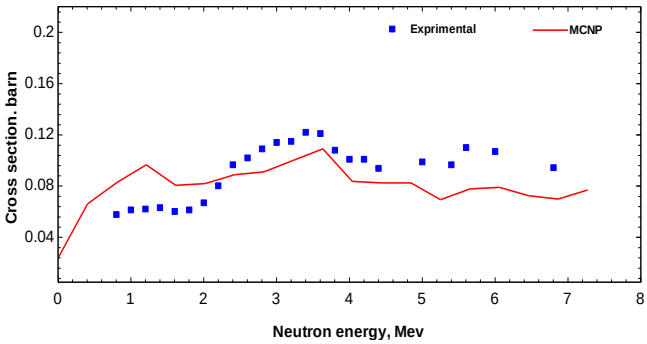

Fig. (9,a) ball clay.

b.sample # 2 (Kawlin) by MCNP simulation

Name	Kawlin
NPS	5E8
Temp.	Room temp
Thickness	2.85cm

Figure. (9.b) depicts the total cross section of fast neutron (Σ) for kawlin calculated by MCNP simulations and measured experimentally which is attributed mostly to inelastic scattering by high density element such as iron through the equation (3). It is observed also that the total cross section mostly depends on the inelastic scattering type and the difference from the above case of the ball clay resulted from the difference in densities of heavy elements composite the shielding material.

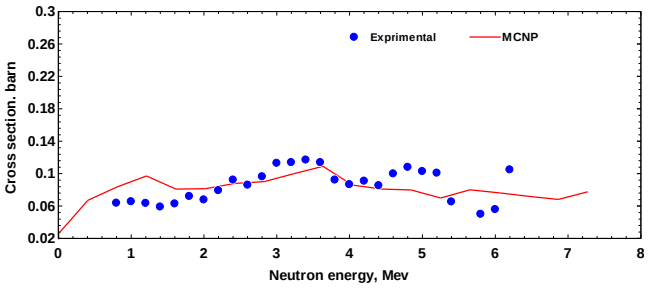

Fig. (9-b) kawlin

c.sample # 3 (Bentonite) by MCNP simulation

Name	Bentonite
NPS	5E8
Temp.	Room temp
Thickness	2.6 cm

Figure. (9.c) shows the total macroscopic cross section of fast neutron (Σ) for Bentonite shields which have been calculated by MCNP simulations and measured experimentally. Also as in the previous two cases is attributed mostly to the inelastic scattering by high density elements composing the shield material (as iron). It is also observed that in addition to the total cross section mostly depends on the inelastic scattering type there is a difference from the above two cases of the ball clay and kawlin which is due to difference in densities of elements composite the shielding sample.

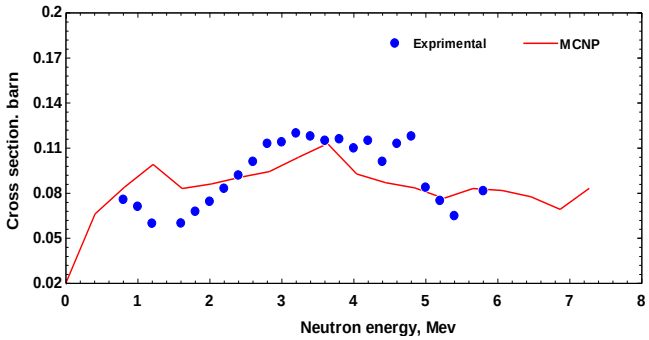

Fig. (9-c).

5 Conclusion

The results show that the total cross section depends on the chemical composition and density of the shielding materials. The shields containing iron with high concentrations in their composition are more effective for attenuation of fast neutrons through inelastic scattering.The total macroscopic cross sections of the samples which calculated by MCNP simulations and measured experimentally verify that the three different samples of clay's have better fast neutron attenuation capabilities. Generally speaking, the results of the experiments and the MCNP simulations are whoevers in agreement with some deviations. -Where the simulation results frequently fall short of those obtained through measurement- which Perhaps due to the assumptions and simplifications made in the simulation geometry. Besides, the difference between the measured and simulated results could be caused by the inhomogeneity composition of the clay samples used in the experiment other than that calculated in Monte Carlo simulation. Furthermore, the difference between results of calculations and experiments may be caused by MCNP simulations itself via the following reasons

1-Simulated material densities and compositions.

2- Uncertainties in the MCNP nuclear data libraries used.

2-The approximation in the model.

3-uncertainty in the measurements and calculations results due to the errors.

References

[1] Y. Elmahroug, B. Tellili, C. Souga, "Determination of shielding parameters for different types of resins, "Tunis: Annals of Nuclear Energy., **63**, 619 – 623, 2014.

[2] G.C., Squires, "Thermal Neutron Scattering," Cambridge University Press., 36 –70, 1978.

[3] E. S. A. Waly and M. A. Bourham, "Comparative study of different concrete composition as gamma-ray shielding materials," Ann. Nucl. Energy., **85**, 306–310, 2015.

[4] B. Oto, N. Yildiz, T. Korkut, and E. Kavaz, "Neutron shielding qualities and gamma ray buildup factors of concretes containing limonite ore," Nucl. Eng. Des., **293**, 166–175, 2015.

[5] D. Jóźwiak-Niedźwiedzka, K. Gibas, A. M. Brandt, M. A. Glinicki, M. Dąbrowski, and P. Denis, "Mineral

Composition of Heavy Aggregates for Nuclear Shielding Concrete in Relation to Alkali-silica Reaction," Procedia Eng., **108**, 162–169, 2015

[6] RM El-Sharkawy, EA Allam, A. El-Taher, ER Shaaban, ME Mahmoud., Synergistic effect of nano-bentonite and nanocadmium oxide doping concentrations on assembly, characterization, and enhanced gamma-rays shielding properties of polypropylene ternary nanocomposites. International Journal of Energy Research., **45(6)**, 8942-8959. 2021.

[7] S., Gladstone, A., Sisonke, "Nuclear Reactor Engineering: Reactor Designs Basic, " New York: Chapman & Hall, Inc., **1**, 59–71,1998.

[8] RM El-Sharkawy, EA Allam, A. El-Taher, R Elsaman, EES Massoud, Mohamed E Mahmoud., Synergistic effects on gamma-ray shielding by novel light-weight nanocomposite materials of bentonite containing nano Bi2O3 additive. Ceramics International., **48(5)**, 7291-7303. 2022.

[9] E Glenn Knoll, Radiation Detection and Measurement. United States of America: John Wiley & Sons Inc., Third Edition, 2000.

[10] Daria J. N., and Lessing, P.A. (2019) High-density and radiation shielding concrete, Woodhead Publishing Series in Civil and Structural Engineering., 193-228, 2019.

[11] Aygün, B. High alloyed new stainless steel shielding material for gamma and fast neutron radiation. Nucl. Eng. Technol., **52**, 647–653, 2020 .

[12] D. Rezaei-Ochbelagh and S. Azimkhani, "Investigation of gamma-ray shielding properties of concrete containing different percentages of lead," Appl. Radiat. Isot., **70(10)**, 2282–2286, 2012.

[13] H. E. Hassan, H. M. Badran, A. Aydarous, and T. Sharshar, "Studying the effect of nano lead compounds additives on the concrete shielding properties for -rays, Nucl. Instruments Methods Phys. Res. Sect. B Beam Interact. with Mater. Atoms., **360**, 81–89, 2015.

[14] S. J. Stanković, R. D. Ilić, K. Janković, D. Bojović, and B. Lončar, "Gamma Radiation Absorption Characteristics of Concrete with Components of Different Type Materials," ., **117(5)**, 812–816, 2010.

[15] M. E. Medhat"Comprehensive study of photon attenuation through different shielding materials.

[16] R. Küçer and N. Küçer "Neutron Shielding Properties of Concretes Containing Boron Carbide and Ferro – Boron.," **195**, 1752–1756, 2015.

[18] O. Gencel, A. Bozkurt, E. Kam, and T. Korkut, "Determination and calculation of gamma and neutron shielding characteristics of concretes containing different hematite proportions," Ann. Nucl. Energy., **38(12)**, 2719–2723, 2011.

[19] I. Akkurt, C. Basyigit, S. Kilincarslan, and B. Mavi, "The shielding of rays by concretes produced with barite," Prog. Nucl. Energy., **46(1)**, 1–11, 2005.

[20] A. El-Taher, HMH Zakaly, M Pyshkina, EA Allam, RM El Sharkawy, Mohamed E Mahmoud, Mohamed AE Abdel-Rahman., A comparative study between Fluka and micro shield modeling calculations to study the radiation-shielding of nanoparticles and plastic waste composites. Zeitschrift für anorganische und allgemeine Chemie., **647(10)**, 1083-1090. 2021.

[21] Atef El-Taher, AM Ali, YB Saddeek, R Elsaman, H Algarni, KS Shaaban, T.Z Amer Gamma ray shielding and structural properties of iron alkali alumino-phosphate glasses modified by PbO. Radiation Physics and Chemistry., **165**, 108403, 2019.

[22] Y.B. Saddeek, K.H.S. Shaaban, Reda Elsaman, Atef El-Taher, T.Z. Amer Attenuation-density anomalous relationship of lead alkali borosilicate Glasses Radiation Physics and Chemistry., **150**, 182–188, 2018.

[23] Dong, M.; Xue, X.; Yang, H.; Liu, D.; Wang, C.; Li, Z. A novel comprehensive utilization of vanadium slag: As gamma ray shielding material. Book

[24] John r. lamarsh, Introduction to nuclear engineering, 1982.